Virology 521 (2018) 190–197

Contents lists available at ScienceDirect

Virology

journal homepage: www.elsevier.com/locate/virology

Molecular evolution of fibropapilloma-associated herpesviruses infecting juvenile green and loggerhead sea turtles

Matthew F. Lawrance[a,b], Katherine L. Mansfield[a], Emma Sutton[a], Anna E. Savage[a,*]

[a] Department of Biology, University of Central Florida, 4110 Libra Drive, Orlando, FL 32816, USA
[b] School of Biological Sciences, Washington State University, Pullman, WA 99613, USA

ARTICLE INFO

Keywords:
Disease ecology
Viral genetics
Asymptomatic carriage
Chelonia mydas
Caretta caretta

ABSTRACT

Chelonid Alphaherpesvirus 5 (ChHV5) has long been associated with fibropapillomatosis (FP) tumor disease in marine turtles. Presenting primarily in juvenile animals, FP results in fibromas of the skin, connective tissue, and internal organs, which may indirectly affect fitness by obstructing normal turtle processes. ChHV5 is near-universally present in tumorous tissues taken from affected animals, often at very high concentrations. However, there is also considerable asymptomatic carriage amongst healthy marine turtles, suggesting that asymptomatic hosts play an important role in disease ecology. Currently, there is a paucity of studies investigating variation in viral genetics between diseased and asymptomatic hosts, which could potentially explain why only some ChHV5 infections lead to tumor formation. Here, we generated a database containing DNA from over 400 tissue samples taken from green and loggerhead marine turtles, including multiple tissue types, a twenty year time span, and both diseased and asymptomatic animals. We used two molecular detection techniques, quantitative (q)PCR and nested PCR, to characterize the presence and genetic lineage of ChHV5 in each sample. We found that nested PCR across multiple loci out-performed qPCR and is a more powerful technique for determining infection status. Phylogenetic reconstruction of three viral loci from all ChHV5-positive samples indicated widespread panmixia of viral lineages, with samples taken across decades, species, disease states, and tissues all falling within the same evolutionary lineages. Haplotype networks produced similar results in that viral haplotypes were shared across species, tissue types and disease states with no evidence that viral lineages associated significantly with disease dynamics. Additionally, tests of selection on viral gene trees indicated signals of selection dividing major clades, though this selection did not divide sample categories. Based on these data, neither the presence of ChHV5 infection nor neutral genetic divergence between viral lineages infecting a juvenile marine turtle is sufficient to explain the development of FP within an individual.

1. Introduction

Family Herpesviridae represents a diverse group of large-DNA icosahedral viruses with widespread host distribution throughout animal lineages, including avian, mammalian, and reptilian hosts (Davison et al., 2009). Extensive efforts to classify associations between herpesvirus and host have produced three broad groupings: alpha-, beta- and gamma-herpesvirus. Of herpesviruses, Alphaherpesviruses are the most specieous, widely distributed amongst host species (Davison, 2000), and tend to coevolve with their hosts (Severini et al., 2013; McGeoch et al., 2000). This coevolution consequently leads to specialization on hosts, resulting in lethal spillover events (Huff and Barry, 2003; Huemer et al., 2002), host-specific transmission routes (including sexual, mechanical, and vectored), and system-specific host symptoms (Whitley and Roizman, 2001a; Gershon et al., 2015). Of note, Alphaherpesviruses are frequently implicated in tumorigenesis of host tissues (Goldberg, 1981; Whitley and Roizman, 2001b). Herpesviruses, such as Epstein-Barr, frequently cause large chromosomal rearrangements when inserting into host genomes (Gerber et al., 1969), and other cellular mechanisms induced by herpesvirus infection can result in tumor formation (Cavallin et al., 2014). Herpesvirus-associated tumor formation is known in many disease systems, including reptilian hosts. Of the reptilian herpesviruses, Alphaherpesviruses in testudinids are phylogenetically basal (McGeoch et al., 2006). This old lineage of herpesvirus is diverse, with novel divergent strains found across numerous host species (Sim et al., 2015; Bicknese et al., 2010; Ossiboff et al., 2015): one of which is strongly associated with tumor formation.

Fibropapillomatosis (FP) is the only known example of a widespread herpsvirus-associated tumorigenic disease in a reptile. FP is a neoplastic tumor disease of marine turtles that presents as fibropapillomas of the

* Corresponding author.
E-mail address: anna.savage@ucf.edu (A.E. Savage).

https://doi.org/10.1016/j.virol.2018.06.012
Received 18 April 2018; Received in revised form 21 June 2018; Accepted 22 June 2018
Available online 28 June 2018

epidermal tissues, and fibromas of the internal organs (Herbst, 1994). Most affected individuals are neritic (coastal) juveniles and subadults, with FP prevalence declining prior to sexual maturity (National Research Council, 1990). Tumors are benign, though biological processes such as digestion, locomotion, and vision may be seriously impaired via obstruction (Herbst, 1994; Brooks et al., 1994a). Severe cases of FP have additionally been linked to increased risk of bacteremia (Brooks et al., 1994b). While green sea turtles (*Chelonia mydas*) are most commonly affected by FP, all marine turtles are capable of contracting the disease (Herbst, 1994). Despite the conservation implications this disease might have for these endangered and threatened species, there are still many unresolved questions pertaining to the disease ecology of FP and its marine turtle hosts.

The putative etiological agent of FP is Chelonid Alphaherpesvirus 5 (ChHV5) (Quackenbush et al., 1998). A genome of 132,233 bp was sequenced and assembled, identifying ChHV5 as a novel genus within Alphaherpesvirus (Herbst et al., 2004), and a suite of molecular markers facilitated numerous phylogenetic analyses (Ene et al., 2005; Greenblatt et al., 2005; Quackenbush et al., 2001). Recently, efforts to culture ChHV5 were successful (Work et al., 2009). Though viral evolution rates, ancient origins of the virus, and co-divergence with host species were demonstrated (Gerber et al., 1969), ecological and genetic variables important for disease progression are still being studied. ChHV5 was initially implicated in FP via histological investigations (Jacobson et al., 1991). These results were further confirmed with the advent of sequencing technology, as fibromas are consistently found to harbor ChHV5 viral DNA (Quackenbush et al., 1998). However, transmission pathways for this virus are still largely unknown, with hypotheses ranging from mechanical, vertical, and leech vectored, though cell-free extract has proven infectious in cell cultures (Herbst et al., 1995).

Most investigations interested in sequence data from ChHV5 rely on samples sourced from tumors or the skin immediately adjacent to tumors (Ene et al., 2005; Patrício et al., 2012). The high concentration of viral DNA in these tissues simplifies the process of amplification, making them attractive targets. Conversely, investigations interested in presence or absence of ChHV5 in asymptomatic animals by necessity utilize non-tumorous tissues, where lower viral concentrations have required the use of more intensive amplification efforts via nested PCR to enhance the likelihood of detection (Herrera et al., 1998; Lu et al., 2000). Detection of ChHV5 in healthy turtles is often as low as 15%, though disentangling low asymptomatic carriage from low probability of detection (i.e., false negatives) remains challenging (Alfaro-Núñez et al., 2016). Due to the differing methods employed in ChHV5 sequencing and detection studies, there is a paucity of information pertaining to viral sequence variation in asymptomatic hosts, save for a few notable studies (Alfaro-Nunez et al., 2014; Page-Karjian et al., 2015). However, such investigations are necessary for understanding the relationship between viral infection and FP, as viral variation may explain why asymptomatic and tumorous hosts can both arise following ChHV5 infection.

Asymptomatic carriers of ChHV5, by definition, cannot be distinguished from non-carriers without molecular analyses and extensive sample collection, presenting a challenge for understanding viral dynamics outside of tumorous hosts. Additionally, asymptomatic tissue often produces inconsistent gene amplification results across viral loci, ostensibly due to low viral DNA concentrations (Page-Karjian et al., 2012). Intensive sampling efforts of many individual turtles are therefore necessary to ensure adequate numbers of sequences for downstream analyses. However, most ChHV5 sequencing studies sample only a few individuals due to challenges associated with sampling large numbers of sea turtles, and consequently do not obtain a large number of viral sequences (Stacy et al., 2008; Rodenbusch et al., 2012). Limitations on sample size is thus a major ongoing challenge for understanding ChHV5 epidemiology in juvenile sea turtles.

Here, we utilize a robust long-term dataset characterizing FP in juvenile marine turtles from 1983 to the present in a well-documented juvenile developmental habitat, the Indian River Lagoon adjacent to the central Atlantic coast of Florida, USA (Abreu-Grobois et al., 2000). This dataset, collected by the University of Central Florida Marine Turtle Research Group (UCF MTRG), represents one of the longest in-water studies for juvenile *C. mydas* and loggerhead (*Caretta caretta*) sea turtles in the US. An average of 145 *C. mydas* juveniles are captured annually, and approximately half of these turtles have visible tumors (Hirama and Ehrhart, 2007). We sampled normal skin, blood and tumors (when present) from asymptomatic and symptomatic *C. mydas* and *C. caretta* turtles over twenty years (1998–2017) to evaluate the relationship between FP dynamics and herpesvirus evolution within turtle tissues, including tissue from numerous asymptomatic individuals. Specifically, we sequenced a suite of three herpesvirus genes (Capsid Maturation Protease *cap*, DNA polymerase catalytic subunit *pol*, and glycoprotein b *glyb*) (Page-Karjian et al., 2012) and used phylogenetic and haplotype analysis to determine whether viral genetic lineages associate with species, tissue types, time periods, or development of FP. We quantified positive natural selection acting within each viral gene to determine if selection drives diversification of viral lineages across different classes of turtle hosts. Additionally, we used quantitative (q)PCR to compare herpesvirus infection intensity among tissues, species and asymptomatic compared to FP individuals. Finally, we compared the efficacy of PCR and qPCR approaches for detecting herpesviruses across marine turtle species and tissues, as well as among viral genetic lineages. Together these analyses provide comprehensive insight into ChHV5 strain relationships in marine turtles with and without FP, as well as a robust assessment of the efficiency of common surveillance and monitoring techniques.

2. Material and methods

2.1. Study site and sample collection

We collected tissue samples from all *C. mydas* and *C. caretta* captured during bi-monthly in-water sampling trips in the Indian River Lagoon (1998–2017). These species regularly occur sympatrically both in this site and throughout their respective ranges, and are known to hybridize (James et al., 2004). Our study site is located approximately 1–2 km south of the Sebastian Inlet within the Indian River Lagoon, Florida (27.8324°N; 80.4420°W). Turtles were captured by large-mesh tangle nets during bi-monthly sampling trips. Nets were set for approximately three hours per sampling session, and tended continuously by boat while soaking. Captured turtles were immediately brought onboard and transferred to a larger work-up boat. Turtles were tagged with flipper and PIT (Passive Integrated Transponder) tags, and standardized morphometrics and weights were collected from each turtle (Bjorndal et al., 1999). Any tumor-like growths indicative of FP were photographed and documented using a standardized scoring system (Balazs and Pooley, 1991): Category 0 – no symptoms, Category 1 – mildly afflicted, Category 2 – moderately afflicted, and Category 3 – severely afflicted. Category scores are subjectively determined by the size, number, and location of the tumors present on the turtles (Work and Balazs, 1999) and the majority of animals with FP in this study were Category 1. Blood was drawn from the dorsal cervical sinus of each turtle into evacuated blood collection tubes using antiseptic protocol and 20-gauge or 22-gauge needles depending on size of the turtle. We collected tissue biopsies following protected species permitted protocols. Each asymptomatic turtle (without FP) was sampled singularly. Any turtle with FP had an additional tissue biopsy taken directly from the most severe tumor observed in order to compare herpesvirus presence and quantity in tumorous versus non-tumorous tissue. The area biopsied was first scrubbed with an isopropyl alcohol swab. The skin biopsy was obtained using a 4-mm sterile biopsy punch. If needed, a coagulant powder was used to control bleeding after tissue sampling. Non-tumor skin samples were taken from the fleshy (non-scale) portion

of the trailing edge of one of the rear flippers. For turtles with FP, a tumor skin sample was collected from the surface of the tumor (i.e., not digging down, but going across the tumor with one side of the biopsy punch, to avoid excessive bleeding). Tissue samples were preserved in 70% ethanol (skin and tumor) or heparinized tubes and transported to the laboratory where they were stored at −20 °C. All captured turtles were released in the vicinity of their capture.

2.2. DNA extraction

A total of 566 samples were extracted utilizing Qiagen DNeasyTM spin columns (Qiagen, Redwood City, California) with the recommended protocol. Approximately 5 mg of skin tissue or 10 μL of blood were utilized in each extraction. Samples were eluted to a standard volume of 200 μL in order to preserve viral comparisons across samples. Extracted samples were stored at −20 °C for future analyses.

2.3. Quantitative PCR

Quantitative PCR was performed with primers, probes, and thermal cycler conditions targeting the pol gene of ChHV5 as previously described (Quackenbush et al., 2001). Reaction conditions were as follows: 8 μL Biorad SSoProbe Supermix (Biorad, Hercules, California), 1 μM each forward and reverse primers, 250 pM probe, with molecular H2O bringing the total reaction volume to 20 μL. Reactions were run on a Biorad CFX 96 thermal cycler, and compared to GeneBlock Standards (IDTDna, Coralville, Iowa) of known concentrations designed to be identical to the targeted pol region in order to quantify viral genome copy number. QPCR results were analyzed using the BioRad CFX software to determine qPCR efficiency, viral presence, and viral load (gene copies). Negative samples and known positives were included in reaction plates in order to confirm assay specificity and control for potential contamination. Reactions demonstrating a cycle of quantification (CQ) earlier than 38 were considered positive (a conservative approach versus the MIQE recommendation of CQ 40). Positive samples were run in duplicate to confirm results, and inconsistent results were run in triplicate and the majority result taken as true. Samples confirmed as positive were utilized for Sanger sequencing. To calculate significance between viral titres across species and tissue samples, duplicate runs were averaged and compared with a Welch's two sided *t*-test accounting for increased variance amongst highly infected tissue types (ie, tumors, $\alpha = 0.05$) to determine significant difference between viral copy means.

2.4. PCR and sanger sequencing

Four loci representing partial gene fragments were targeted for sequencing efforts: 366 bp of DNA polymerase (pol), 333 bp of capsid maturation protein (cap), 309 bp of glycoproteinB (gly) and 711 bp of Serine Threonine Kinase (STK). Three previously designed nested PCR protocols for the target loci cap, pol, and glyb were utilized for all samples (Page-Karjian et al., 2012), in addition to a non-nested PCR for STK. As nested PCR is shown to outperform qPCR in tests of detection in asymptomatic tissue (Herbst et al., 1995), all 566 samples in the dataset, including those negative for qPCR were screened via nested assays. An additional five samples known to contain ChHV5 (MTRG, unpublished) sampled from the 1998 season were provided and included in downstream analyses. PCR reaction conditions were as follows: 1 × OneTaq standard reaction buffer (NewEngland Biolabs, Ipswich, Massachusetts), 200 μM dNTPs, .2 μM forward and reverse primers, .75 U One Taq DNA polymerase, with molecular H2O bringing final reaction volumes to 10 μL. For the first step of nested PCRs (cap, pol, glyb), 3 μL of sample were utilized. 1 μL of PCR product was utilized as template in the second step reaction. Thermal cycler conditions for nested PCR loci were as follows: denaturation for 5 min at 95 °C, followed by 38 cycles of denaturation at 95 °C for thirty seconds, annealing at 50 °C for 30 s, extension at 72 °C for one minutes with a final extension step of 72 °C for two minutes. Thermal cycler conditions for Serine Threonine Kinase were identical, save for annealing at 62 °C.

Amplicons were purified utilizing FastAP and Exonuclease I (FisherSci, Hampton, New Hampshire), and Sanger Sequenced at Eurofins Genomics (Louisville, Kentucky). Chromatograms were visualized and edited by eye in Geneious vs 9.1.6. Consensus sequences were aligned utilizing CLUSTALW (gap penalty: 15, extend penalty: 6.66). Sequencing revealed that all tumors were fixed at the same STK haplotype, thus STK was removed from downstream analyses. The three remaining genes were concatenated and aligned utilizing a similar approach.

2.5. Phylogenetic reconstruction

Models of evolution were determined in PartitionFinder v.2 (Lanfear et al., 2017), SUPPLEMENTAL], partitioning the complete concatenated alignments by gene fragment and codon (3 genes x 3 codon positions for nine total partitions). Models of evolution were selected using Bayesian Information Criterion (BIC). Phylogenies were constructed for both the complete species-tree, as well as independent gene-trees for each locus. Phylogenies were rooted by use of Chelonid Aphlaherpesvirus 6 (LET), a closely related virus that also causes disease in marine turtles. Phylogenetic analyses were conducted via MCMC in BEAST v. 1.8.4 (Drummond et al., 2012). Analyses were run for 10,000,000 iterations with the first 1000 trees (10%) discarded as burn in. Tracer v.1.6 (Rambaut et al., 2014) was used to visualize the convergence of independent chains and determine that effective sample sizes of our parameters were appropriate (> 100). Trees were summed in Tree Annotator (Drummond et al., 2012), specifying the target tree as the sample with the maximum product of posterior clade probabilities. This tree was edited in Figtree v 1.4.3. Post processing was performed in InkScape 0.91.

2.6. Selection analysis

We tested for positive and negative selection using Hypothesis testing using Phylogeny (HyPhy) (Pond and Muse, 2005) implemented on the Datamonkey server (Pond and Frost, 2005). Because selection analyses can be inaccurate in the presence of recombination (Kosakovsky Pond et al., 2006), these analyses were only performed on the independent gene-trees for *gly, pol, and cap* and with the HyPhy-selected nucleotide substitution models for each gene. We further tested for intragenic recombination using GARD (Genetic Algorithms for Recombination Detection) and SBR (Single Breakpoint Recombination), and we only conducted analyses on non-recombining blocks (Kosakovsky Pond et al., 2006). We used PARRIS (PARtitioning approach for Robust Inference of Selection) to detect gene-wide selection (Delport et al., 2010), as well as the six codon-based maximum likelihood approaches to test for site-specific selection, including FEL (Fixed Effects Likelihood), iFEL (internal-FEL), FUBAR (Fast Unconstrained Bayesian AppRoximation), REL (Random Effects Likelihood), SLAC (Single Likelihood Ancestry Counting), and MEME (Mixed Effects Model of Evolution), which only allows testing for positive selection. Significance was set at P-value < 0.05 or Posterior Probability > 0.99, depending on the statistical framework of the site-specific method. Only codons that were found to be under significant positive selection based on at least two of the six site-specific tests were considered to have robust evidence of positive selection.

2.7. Population genetics

We constructed an independent haplotype network of the polymerase locus, the most frequently amplified locus across our dataset, in order to determine the non-recombining ancestry of viral lineages in this study. Population networks of this gene were built utilizing TCS

Table 1
ChHV5 loci that were successfully amplified and Sanger sequenced across different sea turtle tissue types. Only samples that amplified for at least one locus are shown.

		Percent amplification per ChHV5 locus			
Tissue	*No. samples*	*Cap*	*Gly*	*Pol*	*STK*
Tumor	24	79%	93%	95%	88%
Skin	22	56%	78%	91%	4%
Blood	17	5.8%	53%	82%	0%

Table 2
Rates of detection for assays used in this study. Relative qPCR detection is the proportion of qPCR positives recovered compared to nested PCR positives. Denoted by the asterisk, tumor amplification was disproportionately more successful than other tissue types (95% CI 43.9–82.49% for tumors vs −4–15%/-3–27% for ski and blood respectively).

	Total dataset	*No. qPCR positive*	*Percent qPCR positive*	*No. nested PCR positive*	*Percent nested PCR positive*	*Relative qPCR efficacy*
No. samples	566	40	7.1%	64	11.3%	62.50%
Tissue						
Skin	389	13	3.3%	22	5.7%	59.09%
Blood	139	8	5.8%	17	12.2%	47.05%
Tumor	38	19	50.0%	24	63.2%*	79.17%
Species						
C. mydas	463	35	7.6%	57	12.3%	61.40%
C. caretta	103	5	4.9%	7	6.8%	71.43%
Disease state						
Asymptomatic	370	7	1.9%	20	5.4%	35.00%
Tumorous	196	33	16.8%	44	22.4%	75.00%
Sample Year						
2010	83					

(Clement et al., 2002) as implemented in PopArt (Leigh and Bryant, 2015). Trait values were assigned based on species, tissue, year, and disease state of samples.

3. Results

Our final dataset was comprised of 357 and 96 samples of *C. mydas* and *C. caretta* respectively. Samples included blood (n = 139), skin (n = 282) and tumor (n = 32) tissues. A total of 64 out of 566 *C. mydas* and *C. caretta* tissue samples amplified using nested PCR for at least one of four ChHV5 loci (Table 1), and produced high-quality Sanger sequences that were confirmed via homology to sequences in the NCBI nr database to be ChHV5. Viral detection using qPCR and nested PCR was uneven, with nested PCR outperforming qPCR across tissues, species and disease states (Table 2). Overall, qPCR had 62.5% efficacy compared to nested pcr, but particularly suffered in cases of non-tumor tissues, with 35% efficacy across all asymptomatic individuals. Comparisons between species (*C. caretta* vs *C. mydas*) were nonsignificant, but across tissues, tumors displayed significantly higher viral titres than skin or blood (Welch two sided *t*-test, $T_{16} = 3.345$, p = .0048, Fig. 1). Mean pairwise distances between all samples are reported (Table S1): all polymorphisms were substitutions, with no indels detected in our sequences.

The most credible tree (Fig. 2) of the entire dataset reconstructed two well-resolved ChHV5 clades with deep divergence. The derived clade contains two polytomies demarcated with moderate support, and includes an admixture of all sample types (species, tissue, disease state, and year). The basal clade shows extensive diversification between samples resulting in well-resolved tips, though no patterns emerged relating to temporal sampling, tissue type, host species or disease state.

While recombination is known to occur across the ChHV5 genome (Morrison et al., 2018), it was not found to confound selection analyses within our three gene fragments. Using our conservative approach requiring consistent results across at least two codon-based statistical methods, selection testing of our independent gene trees identified one codon, amino acid position 100 in the glycoprotein B gene, that had a significant signal of positive selection acting on one viral clade (Fig. 3, red branches). Tests of positive selection indicating selection at this codon (Table 3) were MEME (p = .011, ω > 100) and REL (Bayes Factor = 1293.340, dN/dS = 1.666). The well-supported clade in the glycoprotein B phylogeny where positive selection acted on codon 100 (posterior = 1) is sister to the clade containing most recovered ChHV5 lineages (Fig. 3). While this smaller clade contains no lineages from tumorous samples, it only represents ChHV5 sampled from two *C. mydas* individuals, presenting a challenge for robust interpretation.

TCS network construction recovered five haplotypes, falling in two major groupings that were consistent with the phylogenetic tree (Fig. 4). Viral haplotypes were shared across host disease state and tissue type. Haplotypes that were exclusive to disease type did not cluster together: the most closely related haplotype to these samples were haplotypes shared between diseased and asymptomatic samples.

4. Discussion

By leveraging a large, long-term dataset of juvenile sea turtles with and without FP, this study resolves an important knowledge gap between ChHV5 sequence data in asymptomatic versus symptomatic hosts. Simultaneously, this effort clarifies the effectiveness of different techniques currently employed in ChHV5 surveillance: nested PCR and qPCR. A principal goal of this study was to determine the efficiency of

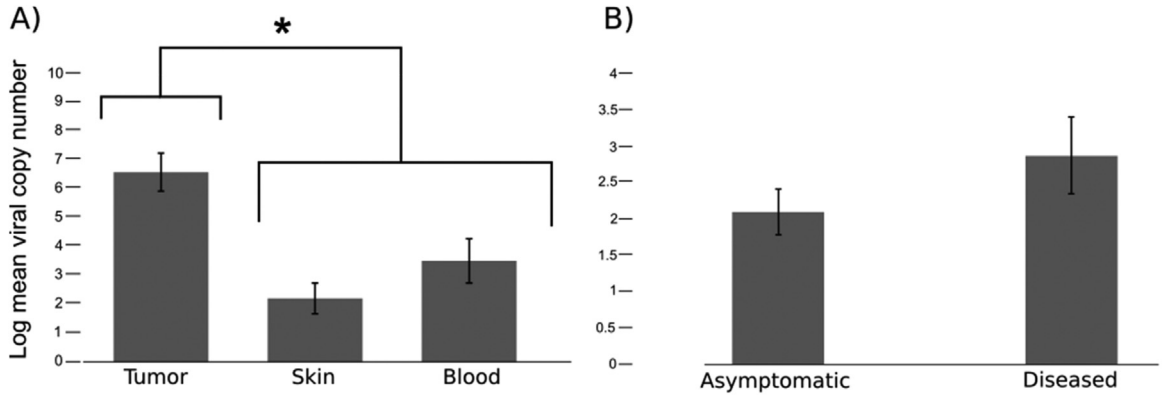

Fig. 1. Infection intensity of herpesvirus infection in tissues recovered in this study, denoted as log number of viral copies for A) Tissue type and B) Disease state. Asterisks denote significantly different comparison between tumorous tissue and asymptomatic tissue (Welch two sided *t*-test, $T_{16} = 3.345$, p = .0048). No significance was found between diseased and asymptomatic individual turtles (p = .218).

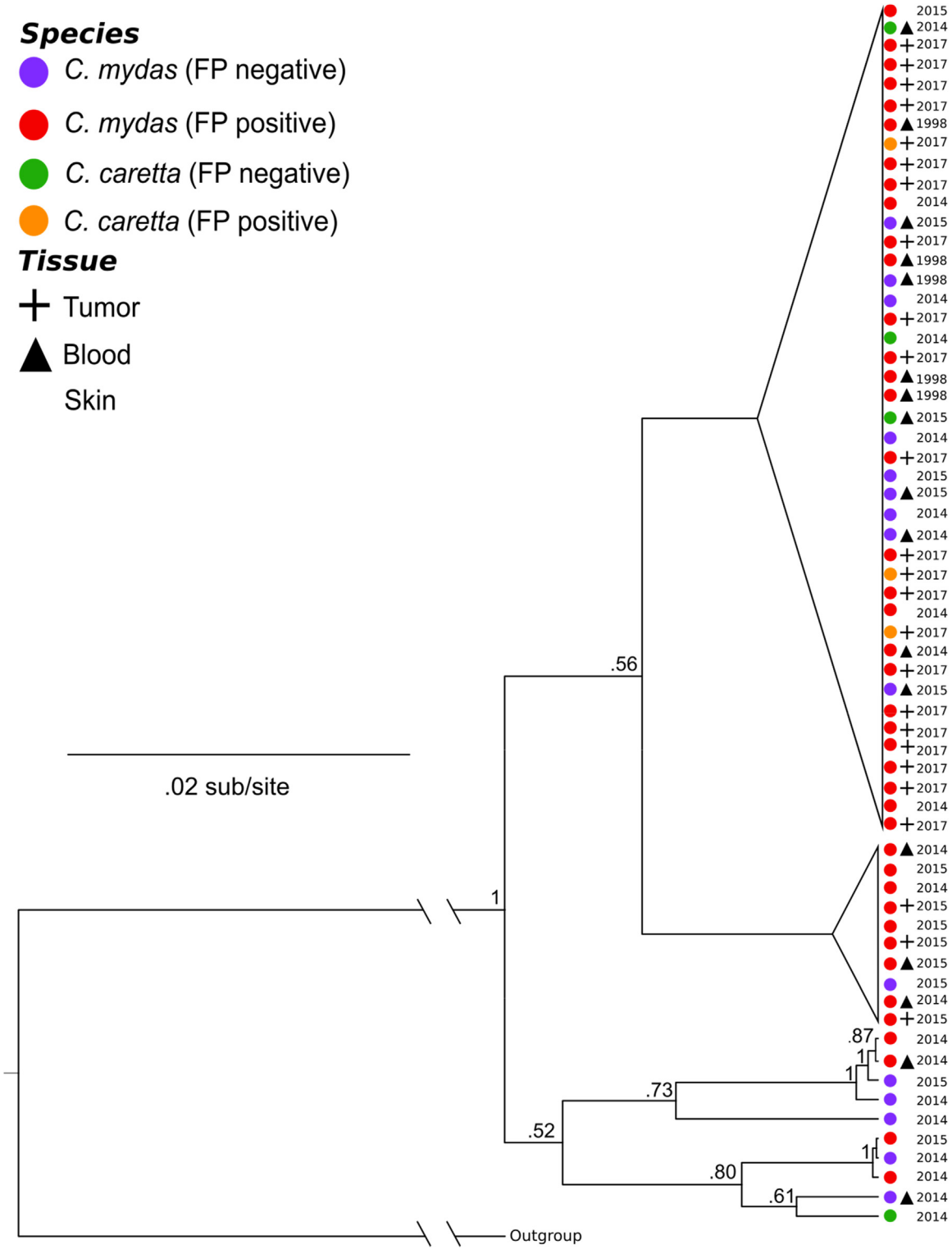

Fig. 2. Phylogenetic reconstruction based on three concatenated loci (*Pol, Cap, Gly),* with outgrouping of *C. mydas* lung and eye herpesvirus spp. Solid circles on nodes denote posterior probabilities of 1. All values above 0.5 are reported. Purple and green tip labels indicate asymptomatic *C. mydas* and *C. caretta* respectively, while red and orange tip labels indicate diseased *C. mydas and C. caretta*, respectively. Tumor and blood are labeled as plus signs and triangles respectively – all remaining unlabeled samples are skin tissue. Phylogenies were constructed via Markov chain Monte Carlo (MCMC) sampling implemented in BEAST.

previously used surveillance tools when specifically applied to low detection probability samples. Universally, nested PCR was a more competent diagnostic tool in recovering positives from our dataset, especially in cases of asymptomatic animals and tissues. The weak detection power from non-tumor samples is of particular importance because the qPCR protocol we utilized was specifically tailored with asymptomatic surveillance as a goal (Quackenbush et al., 2001; Alfaro-Núñez et al., 2016), yet it is these samples in which the discrepancy between techniques is most profound. Despite repeated efforts with high quality reagents (BioRad SSoAdvanced Universal Probe Supermix), qPCR could not be optimized to efficiencies approaching that achieved by nested PCR.

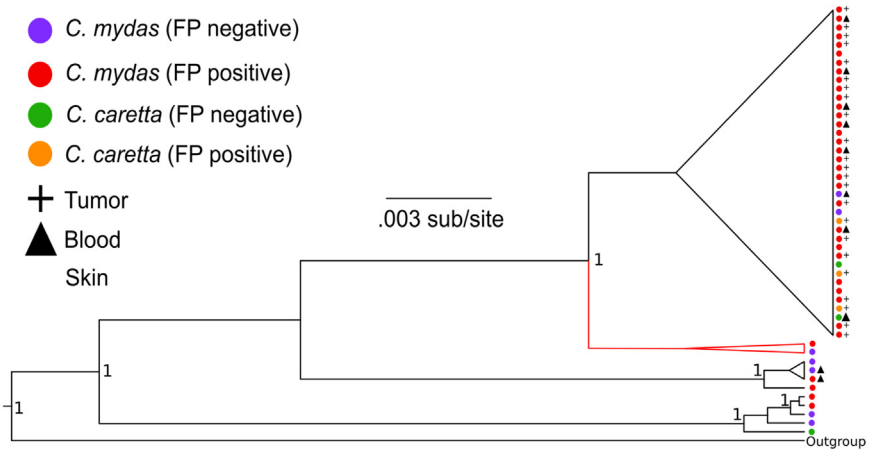

Fig. 3. Phylogenetic reconstruction of Glycoprotein B, with branches under positive selection highlighted in red. Solid circles on nodes denote posterior probabilities of 1. All values above 0.5 are reported. Purple and green tip labels indicate asymptomatic *C. mydas* and *C. caretta* respectively, while red and orange tip labels indicate diseased *C. mydas and C. caretta*, respectively. Tumor and blood are labeled as plus signs and asterisks respectively – all remaining unlabeled samples are skin tissue. Phylogenies were constructed via Markov chain Monte Carlo (MCMC) sampling implemented in BEAST. Signals of selection were detected using the Datamonkey suite of tools.

Table 3
All Glycoprotein B codons under positive selection. All codons were supported by significant BAYES factors via REL. Only one codon (100) was supported at multiple analyses (REL and MEME). Significant Bayes factor (REL)/posterior probability (FUBAR) and p-value (all other analyses) are bolded. Associated dN/dS (REL) and ω (MEME) for significant results are included, italicized.

Codon	SLAC	FEL	REL	MEME	FUBAR
39	0.745	0.542	**638.125** (*1.633*)	0.425	0.689
64	0.792	0.392	**58.330** (*1.091*)	0.670	0.202
100	0.826	0.566	**1293.340** (*1.666*)	**0.011** (> *100*)	0.739
101	0.948	1	**256,883** (*1.700*)	0.271	0.913

The discrepancy among detection techniques is likely because qPCR targets a single locus (polymerase) whereas nested protocols target multiple loci from each tissue sample, with a positive for any locus being indicative of a positive sample. When considering the polymerase gene in isolation as a target for viral detection, nested PCR continued to outperform qPCR in our study (qPCR efficacy versus polymerase nested PCR = 70%). Nested PCR thus combines a more sensitive assay with a multi-locus approach, explaining the markedly higher rates of detection both here and in the original study that developed this assay (Lu et al., 2000). However, the pattern of enhanced detection from nested PCR was not absolute: in rare cases, weakly positive samples for qPCR were not recovered in nested assays. An important caveat is that, in contrast to nested PCR which provides sequence data that confirms unambiguously the presence of ChHV5, qPCR provides no viral sequence data. Both the MIQE qPCR guidelines (Bustin et al., 2009) and empirical disease detection studies (Flori et al., 2004) demonstrate the possibility of weakly positive qPCR results from negative samples resulting in false positives. Thus, a weakly positive qPCR result is potentially the result of spurious amplification, and without sequencing confirmation, we could not definitively consider these samples as positive, despite repeated nested PCR efforts on those samples. Spurious amplification of the qPCR product often resulted in final copy numbers of less than twenty copies even at the final cycle (CQ 40), preventing Sanger sequencing of this off-target product.

Using the sequencing data generated from nested PCR, we incorporated both asymptomatic and tumorous tissues from FP positive and negative individuals to determine if a viral genetic variation might explain patterns in disease ecology. Previous work indicates the need to include asymptomatic tissue in order to determine the role of pathogen genetic variation in disease susceptibility (Alfaro-Núñez et al., 2016), and our study supports this need (Patrício et al., 2012). Our results indicate that diversification of ChHV5 lineages from both asymptomatic and diseased origin is extremely limited, at least within the loci we analyzed. The large polytomy recovered in the concatenated phylogeny included samples from both *C. caretta* and *C. mydas*, and samples from 1998 ranging until 2017, indicating that this clade has remained relatively stable for two decades despite being shared across two host species. Additionally, all clades contained samples from asymptomatic and symptomatic hosts, indicating that viral lineage divergence may play a limited or even no role in disease onset. Notably, only the two poorly-supported, low-divergence polytomies contained samples from tumorous tissue, suggesting that more divergent lineages could be

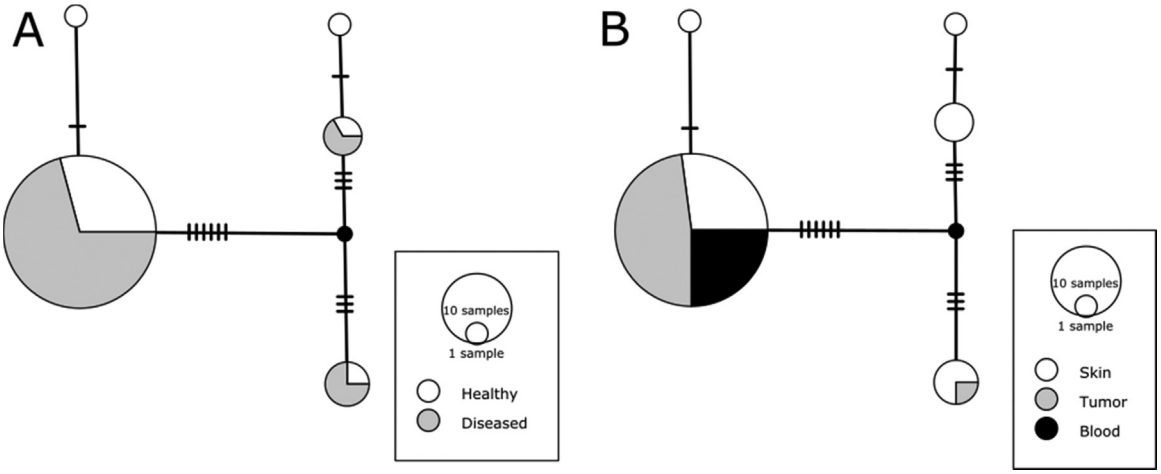

Fig. 4. Haplotype networks for Polymerase gene based on sample traits: A) Diseases verses Healthy hosts B) Tissue type of isolation. Size of circles is indicative of number of samples matching that haplotype. Solid circles and hash marks are representative of inferred mutational steps between haplotypes.

lower virulence lineages linked to lower rates of tumor formation. This is consistent with selection analyses that found positive selection acting only on a lineage without any ChHV5 samples from tumorous tissues. However, small sample sizes and low support values for many lineages within the phylogenies preclude any definitive interpretation. Low posterior support values correspond with the low genetic diversity within the gene fragments incorporated in this study. Therefore, further research, especially including a larger representation of the viral genome, will be necessary to fully resolve patterns of viral evolution and disease associations. Notably, the loci selected in this study are not likely to directly participate in disease onset and represent a nearly neutral cohort for phylogenetic reconstructions capturing viral demography. Were viral lineages diverging respective to their propensity to cause disease, accumulation of variation in neutral loci during this divergence would result in monophyly of these loci respective to the disease trait. The lack of such structure in our phylogeny is indicative that disease is not a trait specific to viral lineage. Future studies explicitly investigating previously implicated oncogenes may clarify relationships that are due to selective forces operating on the disease system (Ackermann et al., 2012), and WGS data derived from newly developed techniques may clarify previously missed background diversification not represented in this dataset.

Given the limited genetic tools currently available for ChHV5, such studies require the development of new resources. While the genome of ChHV5 is sequenced, whole-genome sequencing (WGS) requires isolated genomic tissue from cultured virus (Ackermann et al., 2012), rather than the sparse viral genomic copies interspersed with many turtle genome copies present in tissue extractions from asymptomatic individuals. As whole genome library preparation recommends 500–800 ng of target DNA for successful preparation (NEB UltraNext, New England Biosciences), viral DNA from asymptomatic animals presents a challenge for WGS, as viral genome copies may be as low as a few dozen per microlitre in these samples. The advent of new tools, particularly target capture technology (Warr et al., 2015), and single-cell sequencing (Nawy, 2014) are two approaches that should be implemented to improve our ability to conduct genome-wide analyses of ChHV5 lineages. Metagenomic surveys of asymptomatic and tumorous turtle tissues is also a powerful genomic approach that may further resolve whether other etiological agents, or ChHV5 in combination with other agents, are better predictors of FP than ChHV5 alone. In addition, the improvement of nested PCR and qPCR are also being explored, with enhanced detection rates reported in some cases (Alfaro-Núñez et al., 2016; Page-Karjian et al., 2015).

5. Conclusion

Our data confirms the detectable presence of ChHV5 in three tissue types, including whole blood extractions. Our data indicate that lineage identity of ChHV5 are poor predictors for host disease state, tissue type, temporal effects, or host species. Based on the limited loci assessed here, it appears that the genetics of ChHV5 do not play a significant role in disease progression or diversification, especially as highly similar strains remained constant for the two decades of our sampling. Based on these data, it is likely that some host or environmental processes are at the heart of disease onset and progression.

Acknowledgements

We are grateful to the contribution of many researchers and volunteers who collectively contributed to our sample dataset over several decades, including Dr. L. Ehrhart, D. Bagley, W. Redfoot, and numerous UCF Marine Turtle Research Group interns, students, and volunteers.

Ethics Statement

Sampling was conducted under the University of Central Florida IACUC protocols (14–49W) and federal and state protected species permits (NMFS permit # 19508; FL MTP# 231).

Appendix A. Supporting information

Supplementary data associated with this article can be found in the online version at http://dx.doi.org/10.1016/j.virol.2018.06.012.

References

Abreu-Grobois, F.A., Briseño-Dueñas, R., Sarti-Martínez, L., 2000. Proceedings of the Eighteenth International Sea Turtle Symposium. NOAA Technical Memorandum NMFS-SEFSC-436, (June), 312.

Ackermann, M., Koriabine, M., Hartmann-Fritsch, F., de Jong, P.J., Lewis, T.D., Schetle, N., Leong, J.-A.C., 2012. The genome of chelonid herpesvirus 5 harbors atypical genes. PLoS One 7 (10), 1–15. http://dx.doi.org/10.1371/journal.pone.0046623.

Alfaro-Nunez, A., Bertelsen, M., Bojesen, A., Rasmussen, I., Zepeda-Mendoza, L., Olsen, M., Gilbert, M., 2014. Global distribution of Chelonid Alphaherpesvirus 5 among clinically healthy sea turtles. BMC Evolut. Biol.

Alfaro-Núñez, A., Bojesen, A.M., Bertelsen, M.F., Wales, N., Balazs, G.H., Gilbert, M.T.P., 2016. Further evidence of Chelonid herpesvirus 5 (ChHV5) latency: high levels of ChHV5 DNA detected in clinically healthy marine turtles. PeerJ 4, e2274. http://dx.doi.org/10.7717/peerj.2274.

Balazs, G.H., Pooley, S.G., 1991. Research plan for marine turtle fibropapilloma: results of a December 1990 workshop.

Bicknese, E.J., Childress, A.L., Wellehan, J.F.X., 2010. A novel herpesvirus of the proposed genus chelonivirus from an asymptomatic bowsprit tortoise (Chersina angulata). J. Zoo Wildl. Med. 41 (2), 353–358. http://dx.doi.org/10.1638/2009-0214R.1.

Bjorndal, K.A., Wetherall, J.A., Bolten, A.B., Mortimer, J.A., 1999. Twenty-six years of green turtle nesting at Tortuguero, Costa Rica: an encouraging trend. Conserv. Biol. 13 (1), 126–134.

Brooks, D.E., Ginn, P.E., Miller, T.R., Bramson, L., Jacobson, E.R., 1994a. Ocular fibropapillomas of green turtles (Chelonia mydas). Vet. Pathol. Online 31 (3), 335–339. http://dx.doi.org/10.1177/030098589403100306.

Brooks, D.E., Ginn, P.E., Miller, T.R., Bramson, L., Jacobson, E.R., 1994b. Ocular fibropapillomas of green turtles (Chelonia mydas). Vet. Pathol. Online 31 (3), 335–339. http://dx.doi.org/10.1177/030098589403100306.

Bustin, S.A., Benes, V., Garson, J.A., Hellemans, J., Huggett, J., Kubista, M., Wittwer, C.T., 2009. The MIQE guidelines: minimum information for publication of quantitative real-time PCR experiments. Clin. Chem. 55 (4), 611–622. http://dx.doi.org/10.1373/clinchem.2008.112797.

Cavallin, L.E., Goldschmidt-Clermont, P., Mesri, E.A., 2014. Molecular and cellular mechanisms of KSHV oncogenesis of Kaposi's sarcoma associated with HIV/AIDS. PLoS Pathog. 10 (7), e1004154. http://dx.doi.org/10.1371¬¬¬¬/journal.ppat.1004154.

Clement, M., Snell, Q., Walke, P., Posada, D., Crandall, K., 2002. TCS: estimating gene genealogies. Proc 16th Int Parallel Distrib Process Symp 2:184.

Davison, A.J., 2000. Molecular Evolution of Alphaherpesviruses. Varicella Zoster Virus. Cambridge University Press, Cambridge, England, pp. 25–50.

Davison, A.J., Eberle, R., Ehlers, B., Hayward, G.S., McGeoch, D.J., Minson, A.C., Thiry, E., 2009. The order Herpesvirales. Arch. Virol. 154 (1), 171–177. http://dx.doi.org/10.1007/s00705-008-0278-4.

Delport, W., Poon, A.F.Y., Frost, S.D.W., Kosakovsky Pond, S.L., 2010. Datamonkey 2010: a suite of phylogenetic analysis tools for evolutionary biology. Bioinformatics 26 (19), 2455–2457. http://dx.doi.org/10.1093/bioinformatics/btq429.

Drummond, A.J., Suchard, M.A., Xie, D., Rambaut, A., 2012. Bayesian phylogenetics with BEAUti and the BEAST 1.7. Mol. Biol. Evol. 29 (8), 1969–1973. http://dx.doi.org/10.1093/molbev/mss075.

Ene, A., Su, M., Lemaire, S., Rose, C., Schaff, S., Moretti, R., Herbst, L.H., 2005. Distribution of chelonid fibropapillomatosis-associated herpesvirus variants in Florida: molecular genetic evidence for infection of turtles following recruitment to neritic developmental habitats. J. Wildl. Dis. 41 (3), 489–497. http://dx.doi.org/10.7589/0090-3558-41.3.489.

Flori, P., Bellete, B., Durand, F., Raberin, H., Cazorla, C., Hafid, J., Sung, R.T.M., 2004. Comparison between real-time PCR, conventional PCR and different staining techniques for diagnosing Pneumocystis jiroveci pneumonia from bronchoalveolar lavage specimens. J. Med. Microbiol. 53 (7), 603–607. http://dx.doi.org/10.1099/jmm.0.45528-0.

Gerber, P., Whang-Peng, J., Monroe, J.H., 1969. Transformation and chromosome changes induced by epstein-barr virus in normal human leukocyte cultures. Proc. Natl. Acad. Sci. USA 63 (3), 740–747. (Retrieved from). 〈http://www.pnas.org/content/63/3/740.abstract〉.

Gershon, A.A., Breuer, J., Cohen, J.I., Cohrs, R.J., Gershon, M.D., Gilden, D., Yamanishi, K., 2015. Varicella zoster virus infection. Nat. Rev. Dis. Prim. 1, 15016. http://dx.doi.org/10.1038/nrdp.2015.16.

Goldberg, G.N., 1981. In utero epstein-barr virus (infectious mononucleosis) infection. J. Am. Med. Assoc. 246 (14), 1579. http://dx.doi.org/10.1001/jama.1981.03320140067034.

Greenblatt, R.J., Quackenbush, S.L., Casey, R.N., Rovnak, J., Balazs, G.H., Work, T.M., Sutton, C.A., 2005. Genomic variation of the fibropapilloma-associated marine turtle herpesvirus across seven geographic areas and three host species. J. Virol. 79 (2), 1125–1132. http://dx.doi.org/10.1128/JVI.79.2.1125.

Herbst, L., Ene, A., Su, M., Desalle, R., Lenz, J., 2004. Tumor outbreaks in marine turtles are not due to recent herpesvirus mutations. Curr. Biol. 14 (17), 697–699. http://dx.

doi.org/10.1016/j.cub.2004.08.040.
Herbst, L.H., 1994. Fibropapillomatosis of marine turtles. Annu. Rev. Fish. Dis. 4 (6), 389–425. http://dx.doi.org/10.1016/0959-8030(94)90037-X.
Herbst, L.H., Jacobson, E.R., Moretti, R., Brown, T., Sundberg, J.P., Klein, P.A., 1995. Experimental transmission of green turtle fibropapillomatosis using cell-free tumor extracts. Dis. Aquat. Org. 22 (1), 1–12. http://dx.doi.org/10.3354/dao022001.
Herrera, M.S., Curry, S.S., Brown, D.R., Homer, B.L., Garber, R.L., Mader, D.R., … Lackovichl, J.K., 1998. Prevalence and Cultivation of a Chelonid herpesvirus associated with fibropapillomas of the green turtle, Chelonia mydas, and the longgerhead turtle, Caretta caretta, in Florida. Laboratory Medicine.
Hirama, S., Ehrhart, L.M., 2007. Description, prevalence and severity of green turtle fibropapillomatosis in three developmental habitats on the east coast of Florida. Fla. Sci. 435–448.
Huemer, H.P., Larcher, C., Czedik-Eysenberg, T., Nowotny, N., Reifinger, M., 2002. Fatal infection of a pet monkey with human herpesvirus 1. Emerg. Infect. Dis. 8 (6), 639–641. http://dx.doi.org/10.3201/eid0806.010341.
Huff, J.L., Barry, P.A., 2003. B-Virus (Cercopithecine herpesvirus 1) infection in humans and macaques: potential for zoonotic disease. Emerg. Infect. Dis. 9 (2), 246–250. http://dx.doi.org/10.3201/eid0902.020272.
Jacobson, E.R., Buergelt, C., Williams, B., Harris, R.K., 1991. Herpesvirus in cutaneous fibropapillomas of the green turtle Chelonia mydas. Dis. Aquat. Org. 12 (1), 1–6. http://dx.doi.org/10.3354/dao012001.
James, M.C., Martin, K., Dutton, P.H., 2004. Hybridization between a green turtle, Chelonia mydas, and loggerhead turtle, Caretta caretta, and the first record of a green turtle in Atlantic Canada. Can. Field-Nat. 118 (4), 579–582.
Kosakovsky Pond, S.L., Posada, D., Gravenor, M.B., Woelk, C.H., Frost, S.D.W., 2006. GARD: a genetic algorithm for recombination detection. Bioinformatics 22 (24), 3096–3098. http://dx.doi.org/10.1093/bioinformatics/btl474.
Lanfear, R., Frandsen, P.B., Wright, A.M., Senfeld, T., Calcott, B., 2017. PartitionFinder 2: new methods for selecting partitioned models of evolution for molecular and morphological phylogenetic analyses. Mol. Biol. Evol. 34 (3), 772–773. http://dx.doi.org/10.1093/molbev/msw260.
Leigh, J.W., Bryant, D., 2015. popart: full-feature software for haplotype network construction. Methods Ecol. Evol. 6 (9), 1110–1116. http://dx.doi.org/10.1111/2041-210X.12410.
Lu, Y., Wang, Y., Yu, Q., Aguirre, A.A., Balazs, G.H., Nerurkar, V.R., Yanagihara, R., 2000. Detection of herpesviral sequences in tissues of green turtles with fibropapilloma by polymerase chain reaction. Arch. Virol. 145 (9), 1885–1893. http://dx.doi.org/10.1007/s007050070063.
McGeoch, D.J., Dolan, A., Ralph, A.C., 2000. Toward a comprehensive phylogeny for mammalian and avian herpesviruses. J. Virol. 74 (22), 10401–10406.
McGeoch, D.J., Rixon, F.J., Davison, A.J., 2006. Topics in herpesvirus genomics and evolution. Virus Res. 117 (1), 90–104. http://dx.doi.org/10.1016/j.virusres.2006.01.002.
Morrison, C.L., Iwanowicz, L., Work, T.M., Fahsbender, E., Breitbart, M., Adams, C., Cornman, R.S., 2018. Genomic evolution, recombination, and inter-strain diversity of chelonid alphaherpesvirus 5 from Florida and Hawaii green sea turtles with fibropapillomatosis. PeerJ 6, e4386.
National Research Council, 1990. Decline of the Sea Turtles: Causes and Prevention. National Academy Press, Washington.
Nawy, T., 2014. Single-cell sequencing. Nat. Methods 11 (1), 18.
Ossiboff, R.J., Raphael, B.L., Ammazzalorso, A.D., Seimon, T.A., Newton, A.L., Chang, T.Y., McAloose, D., 2015. Three novel herpesviruses of endangered clemmys and glyptemys turtles. PLoS One 10 (4), e0122901. http://dx.doi.org/10.1371/journal.pone.0122901.
Page-Karjian, A., Torres, F., Zhang, J., Rivera, S., Diez, C., Moore, P.A., Brown, C., 2012. Presence of Chelonid Alphaherpesvirus 5 in tumorous and non-tumorous green turtles, as detected by polymerase chain reaction, in endemic and non-endemic aggregations, Puerto Rico. SpringerPlus 1 (1), 35. http://dx.doi.org/10.1186/2193-1801-1-35.
Page-Karjian, A., TM, N., Ritchie, B., Brown, C., Mancia, C., Jackwood, M., Gottdenker, N.L., 2015. Quantifying chelonid herpesvirus 5 in symptomatic and asymptomatic rehabilitating green sea turtles. Endanger. Species Res. 28 (2), 135–146.
Patrício, A.R., Herbst, L.H., Duarte, A., Vélez-Zuazo, X., Loureiro, N.S., Pereira, N., Toranzos, G.A., 2012. Global phylogeography and evolution of Chelonid alphaherpesvirus 5. J. Gen. Virol. 93 (5), 1035–1045. http://dx.doi.org/10.1099/vir.0.038950-0.
Pond, S.L.K., Frost, S.D.W., 2005. Datamonkey: rapid detection of selective pressure on individual sites of codon alignments. Bioinformatics 21 (10), 2531–2533. http://dx.doi.org/10.1093/bioinformatics/bti320.
Pond, S.L.K., Muse, S.V., 2005. HyPhy: Hypothesis Testing Using Phylogenies. In: Rasmus, Nielsen (Ed.), Statistical Methods in Molecular Evolution. Springer New York, New York, NY, pp. 125–181. http://dx.doi.org/10.1007/0-387-27733-1_6.
Quackenbush, S.L., Work, T.M., Balazs, G.H., Casey, R.N., Rovnak, J., Chaves, A., Casey, J.W., 1998. Three closely related herpesviruses are associated with fibropapillomatosis in marine turtles. Virology 246 (2), 392–399 (https://doi.org/S0042-6822)(98)(99207-8)(pii)(/r10.1006/viro.1998.9207).
Quackenbush, S.L., Casey, R.N., Murcek, R.J., Paul, T.A., Work, T.M., Limpus, C.J., Casey, J.W., 2001. Quantitative analysis of herpesvirus sequences from normal tissue and fibropapillomas of marine turtles with real-time PCR. Virology 287 (1), 105–111. http://dx.doi.org/10.1006/viro.2001.1023/rS0042-6822(01)91023-2. (pii).
Rambaut A., Suchard M.A., Xie D., Drummond A.J., 2014. Tracer v1.6, Available from ⟨http://tree.bio.ed.ac.uk/software/tracer/⟩.
Rodenbusch, C.R., Almeida, L.L., Marks, F.S., Ataíde, M.W., Alievi, M.M., Tavares, M., Canal, C.W., 2012. Detection and characterization of fibropapilloma associated herpesvirus of marine turtles in Rio Grande do Sul, Brazil. Pesqui. Vet. Bras. 32 (11), 1179–1183. http://dx.doi.org/10.1590/S0100-736×2012001100018.
Severini, A., Tyler, S.D., Peters, G.A., Black, D., Eberle, R., 2013. Genome sequence of a chimpanzee herpesvirus and its relation to other primate alphaherpesviruses. Arch. Virol. 158 (8), 1825–1828. http://dx.doi.org/10.1007/s00705-013-1666-y.
Sim, R.R., Norton, T.M., Bronson, E., Allender, M.C., Stedman, N., Childress, A.L., Wellehan, J.F.X., 2015. Identification of a novel herpesvirus in captive Eastern box turtles (Terrapene carolina carolina). Vet. Microbiol. 175 (2), 218–223. http://dx.doi.org/10.1016/j.vetmic.2014.11.029.
Stacy, B.A., Wellehan, J.F.X., Foley, A.M., Coberley, S.S., Herbst, L.H., Manire, C.A., Jacobson, E.R., 2008. Two herpesviruses associated with disease in wild Atlantic loggerhead sea turtles (Caretta caretta). Vet. Microbiol. 126 (1–3), 63–73. http://dx.doi.org/10.1016/j.vetmic.2007.07.002.
Warr, A., Robert, C., Hume, D., Archibald, A., Deeb, N., Watson, M., 2015. Exome sequencing: current and future perspectives. G3: Genes|Genomes|Genet. 5 (8), 1543–1550. http://dx.doi.org/10.1534/g3.115.018564.
Whitley, R.J., Roizman, B., 2001a. Herpes simplex virus infections. Lancet 357 (9267), 1513–1518. http://dx.doi.org/10.1016/S0140-6736(00)04638-9.
Whitley, R.J., Roizman, B., 2001b. Herpes simplex virus infections. Lancet 357 (9267), 1513–1518. http://dx.doi.org/10.1016/S0140-6736(00)04638-9.
Work, T.M., Balazs, G.H., 1999. Relating tumor score to hematology in green turtles with fibropapillomatosis in Hawaii. J. Wildl. Dis. 35 (4), 804–807. http://dx.doi.org/10.7589/0090-3558-35.4.804.
Work, T.M., Dagenais, J., Balazs, G.H., Schumacher, J., Lewis, T.D., Leong, J.A.C., Casey, J.W., 2009. In vitro biology of fibropapilloma-associated turtle herpesvirus and host cells in Hawaiian green turtles (Chelonia mydas). J. Gen. Virol. 90 (8), 1943–1950. http://dx.doi.org/10.1099/vir.0.011650-0.